Thrust of an Air-Augmented Waterjet with a Converging-Diverging Nozzle

Timothy T. Maxwell*
Sperry Rand Corporation, Phoenix, Ariz.

Glennon Maples,† and David F. Dyer‡
Auburn University, Auburn, Ala.

This study is concerned with predicting the performance of an air-augmented waterjet with a converging-diverging nozzle. The device under study is one in which compressed air is injected into the high-pressure water stream leaving the water pump. A mixture of water and finely dispersed air bubbles is generated in a constant-area mixing chamber, which joins the water-pump outlet. The two-phase bubbly mixture enters the converging-diverging thrust nozzle and expands under the action of a negative pressure gradient. The two-phase nozzle flow is analyzed through application of the conservation laws for a single air bubble and an incremental control volume over a nozzle section. Three different models which describe the heat transfer between the air bubbles and the water are considered. Results indicate that thrust augmentation is most effective for low pump-outlet pressures and for high mass flow ratios in the range permitting bubbly flow. The solution of the nozzle flow was accomplished by specifying the velocity distribution in the nozzle and calculating the nozzle geometry. Several expressions were used to calculate sonic velocity and it is shown that discrepancies exist between the computed results of the different expressions. Also none of the expressions place the sonic velocity at the throat. Thus, it is shown that further work is needed in determining sonic speed in two-phase compressible mixtures.

Nomenclature

A = cross-sectional area
C_d = drag coefficient, drag/$\frac{1}{2}\rho_w(V-U)^2\pi r^2$
C_p = specific heat at constant pressure
c = velocity of sound
h_c = average convective heat transfer coefficient
K = ratio of specific heats
k = thermal conductivity
L = nozzle length
ℓ = nozzle radius
M = Mach number
m = mass flow rate
Nu = Nusselt number, $2rh_c/k_w$
P = pressure
Pr = Prandtl number, $\mu_w C_p/k_w$
q = quality
R = gas constant
Re = Reynolds number, $\rho_w 2r(v-U)/\mu_w$
r = bubble radius
T = temperature
U = water velocity
V = air velocity
x = coordinate along center line of nozzle
α = void fraction
μ = dynamic viscosity
ν = mass flow ratio
ρ = mass density
θ = thrust
ϕ = typical property

Subscripts

a = ambient
e = nozzle exit
f = properties evaluated at film temperature
g = air
i = pump-outlet; mixing chamber inlet
m = mixture chamber outlet; nozzle entrance
w = water

Introduction

THIS paper is an extension of the work of Amos[1] and others and is concerned with predicting the performance of an air-augmented water-jet. The basic apparatus under consideration is shown in Fig. 1 where it is seen that the new feature in comparison to a standard water-jet system is the introduction of compressed air which is taken from the prime mover. Reference 1 gives an extensive historical review of waterjet propulsion indicating its advantages and disadvantages. Also an analytical analysis is given which develops the equations applying to a comprehensive model of the mixing chamber and converging thrust nozzle.

The present contribution is to extend the analysis of Ref. 1 to include flow through a converging-diverging thrust nozzle. Further, comparisons of results for various published models for sonic velocity will be shown which exhibit large variation in sonic velocity for the same location in the nozzle. Thus, it is shown that the location of the sonic point cannot be determined accurately with existing models for sonic velocity.

Problem Statement

Figure 2 shows schematically the system to be analyzed. For various inlet conditions (air bubble size, temperature, and pressure; water pressure and temperature; and mass ratio of air to water) it is desired to predict the thrust developed by the nozzle. Further, it is desired to determine if thrust augmentation has been achieved by injection of air. The system is divided into two parts: the mixing chamber and the nozzle. A global analysis of the mixing chamber is required to determine

Received November 11, 1974; revision received April 18, 1975. The authors gratefully acknowledge the support of the Office of Naval Research under Contract N00014-72-C-0177.

Index categories: Multiphase Flows; Marine Propulsion System Integration

*Engineer.

†Associate Professor, Department of Mechanical Engineering. Member AIAA.

‡Associate Professor, Department of Mechanical Engineering.

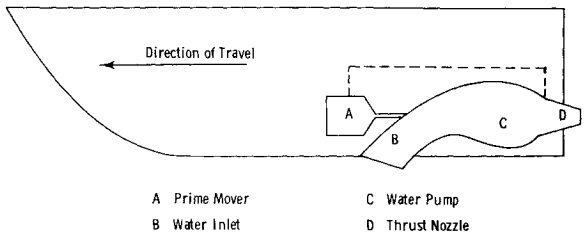

Fig. 1 Typical waterjet installation.

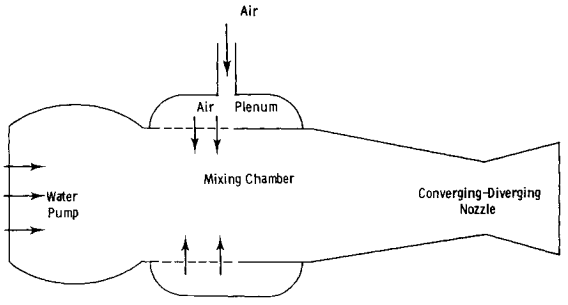

Fig. 2 Schematic diagram of air-augmented waterjet.

the distribution of properties entering the nozzle. A detailed one-dimensional analysis of the compressible flow in the nozzle is required to predict the properties at the exit of the nozzle and thrust produced by the flow.

Since two-phase sonic-velocity models do not accurately predict the sonic velocity, the nozzle cross-sectional area is not a satisfactory independent variable. This is true because inaccuracies in sonic velocity prediction will cause the sonic point to be located away from the throat if it is specified 'a priori,' causing the predicted performance to be significantly in error. Thus, alternate calculation procedures or accurate sonic velocity models must be developed.

Model

Amos[1] developed a comprehensive model applicable to the case under study. The assumptions used are stated following: 1) The flow is steady and quasi one-dimensional at the inlet and outlet of the mixing chamber and throughout the exhaust nozzle. 2) The mixing chamber and nozzle walls are frictionless and thermally nonconductive. 3) The water is incompressible and has a constant temperature throughout the system. 4) The air is a calorically perfect gas. 5) Mass transfer between the gas and water phases is negligible. 6) Air bubbles, formed during the mixing process, pass through the mixing chamber outlet in the form of homogeneously dispersed spheres, each with a velocity equal to the water velocity. 7) The gas pressure in the air bubbles is at each point equal to the local water static pressure. 8) The air bubbles remain spherical during their residence in the nozzle, do not coalesce nor divide, and have a constant value of their radii at any nozzle section. 9) In the exhaust nozzle, heat transfer takes place between the air bubbles and the water only by the process of forced convection. 10) The two fluids in the nozzle have different velocities.

The equations applying to both the mixing chamber and nozzle for this model have been derived by Amos[1] and their development will not be repeated. A summary of the 7 equations for the nozzle is given following.

Nozzle Equations

$$\frac{K}{K-1}PV\frac{dr}{dx}+\frac{1}{K-1}\frac{rV}{3}\frac{dP}{dx}+h_c(T_g-T_w)=0 \quad (1)$$

$$\frac{dP}{dx}+(\rho_g+\rho_w/2)V\frac{dV}{dx}-\rho_w/2\,U\frac{dU}{dx}+\frac{3C_D\rho_w}{8r}(V-U)\,|V-U|=0 \quad (2)$$

$$(1-\alpha)\rho_w U\frac{dU}{dx}+\rho_g\alpha V\frac{dV}{dx}+\frac{dP}{dx}=0 \quad (3)$$

$$\frac{1}{A}\frac{dA}{dx}+\frac{dU}{dx}-\frac{1}{1-\alpha}\frac{d\alpha}{dx}=0 \quad (4)$$

$$\frac{1}{A}\frac{dA}{dx}+\frac{1}{V}\frac{dV}{dx}+\frac{1}{\alpha}\frac{d\alpha}{dx}+\frac{1}{\rho_g}\frac{d\rho_g}{dx}=0 \quad (5)$$

$$\frac{1}{\rho_g}\frac{d\rho_g}{dx}+3/r\frac{dr}{dx}=0 \quad (6)$$

$$\frac{dP}{dx}-\frac{\rho_g R_g dT_g}{dx}-T_g R_g\frac{d\rho_g}{dx}=0 \quad (7)$$

where the air equation of state has been used, namely

$$P=\rho_g R_g T_g \quad (8)$$

Bubble Heat Transfer and Drag Coefficient

Other relationships are required to relate Nusselt number and drag coefficients to Reynolds number. Three models were used for bubble heat transfer: 1) adiabatic, 2) isothermal and 3) an empirical relationship developed by Vliet and Leppert.[2] This third relation is valid for the Reynolds number range $1<Re\times 3\times 10^5$ and is

$$Nu(Pr)^{-0.3}\left[\frac{\mu_w}{\mu_f}\right]^{0.25}=1.2+.53(Re)^{0.54} \quad (9)$$

For low Reynolds numbers, the bubble drag coefficient is taken as that for a solid sphere moving with the bubble relative velocity. The drag coefficient relations and the Reynolds number ranges in which they apply are as follows

$$C_D=24/Re\ (1+3/16\ Re);\ Re\le 2 \quad (10)$$

$$C_D=(18.5/Re^{0.6});2<Re\le 500 \quad (11)$$

$$C_d=0.445+[(Re-500)/181];\ 500<Re\le 600 \quad (12)$$

$$C_D=1;\ 600<Re\le 900 \quad (13)$$

$$C_D=1+[(Re-900)/200];\ 900<Re\le 1200 \quad (14)$$

$$C_D=2.5;\ 1200<Re \quad (15)$$

Equations (10-15) are from Refs. 3-5.

Properties

Expressions for the properties of air and water, such as specific heats, density, Prandtl number, and thermal conductivity, as functions of temperature were obtained by curve fitting data from Kreith[6] and Keenan and Kaye.[7]

Thrust Equation

The thrust developed by the system, when the water enters the mixing chamber at a velocity U_i, and there is no external

acceleration of the water stream, is

$$\theta = m_w(U_e - U_i) + m_g V_e + A_e(P_e - P_a) \tag{16}$$

Mach Number Equations

Numerous expressions for calculating the sonic velocity of a two-phase mixture are available in the literature. Wallis[8] gives the following equation for the velocity of sound in a bubbly mixture

$$c^2 = \frac{1}{(\alpha\rho_g + (1-a)\rho_w)\ (\alpha/\rho_g c^2 g + (1-\alpha)/\rho_w c^2{}_w)} \tag{17}$$

Equation (17) is valid for small bubbles with a density much less than the liquid density. Wallis also gives

$$c = (c_g/[\alpha(1-\alpha)\rho_w/\rho_g]^{1/2}) \tag{18}$$

as an approximation for α greater than 10^{-3}. Van Wijngaarden[9] gives two approximations. The first,

$$c^2 = P/\rho_w\alpha(1-\alpha) \tag{19}$$

is for α not close to zero or unity, and the second,

$$c^2 = (1+2\alpha)KP/\rho_w\alpha(1-\alpha) \tag{20}$$

is for isentropic waves. Henry, Grolmes, and Fauske[10] propose for low qualities, that

$$c^2(\ (1-q)\rho_g + q\rho_w)^2/\left[\frac{q\rho_w{}^3}{c_g{}^2} + \frac{(1-q)\rho_g{}^2}{c_w{}^2}\right] \tag{21}$$

where q is the quality. The Mach number is then calculated by the expression

$$M = (\alpha V + (1-\alpha)U)/c \tag{22}$$

Solution Technique

Reference 1 develops and lists the equations describing the process in the mixing chamber. These form a set of nonlinear, coupled algebraic equations. If the diameter of the mixing chamber entrance and exit, and the conditions of the air and water entering the chamber are specified, this set of equations can be solved for the properties of the fluids leaving the mixing chamber. These properties serve as inlet conditions for the nozzle calculation.

The equations describing flow in the nozzle, Eqs. (1-7), form a set of 7, coupled, first-order, nonlinear differential equations. These 7 equations contain 8 unknowns: pressure, water velocity, air velocity, air temperature, air density, void fraction, bubble radius, and area of the nozzle. Each of the unknown quantities is a function of the distance from the nozzle entrance x. To obtain a solution to this set of equations one of the 8 functions must be specified. Mathematically, it makes no difference which of the unknown functions is specified; however, the physical conditions of the problem suggest specifying the nozzle shape. Even though specifying the nozzle geometry is the most logical way to approach the problem, this method may be used only for converging nozzles. When a converging-diverging shape is specified the input conditions must be picked so that the location of the throat, calculated by the solution process, will coincide with the location specified for the throat. Hence, either the flow will choke before the minimum area is reached and the flow rate will decrease, or the flow will not choke, but will diffuse in the diverging section of the duct.

The velocity profile of the water phase was specified and the system of equations was solved for the remaining properties. Inspection of Eqs. (1-7) shows that Eqs. (1-3, 6, and 7), rewritten with all terms not containing a derivative of P, V, r, T_g, or ρ_g on the right, form a set of linear, coupled, algebraic equations for dP/dx, dV/dx, dr/dx, dT_g/dx. If the properties at x are known, then the derivatives can be calculated at $x+\Delta x$, and hence, the properties, P, V, r, T_g, and ρ_g at $x+\Delta x$ can be calculated by the following equation

$$\phi_{x+\Delta x} = \phi_x + \left.\frac{d\phi}{dx}\right|_x \Delta x \tag{23}$$

Equations (4) and (5) are used to calculate A and α. After integration with respect to x, Eqs. (4) and (5) can be written

$$\rho_g \alpha A V = m_g = \text{flow rate of air} \tag{24}$$

$$\rho_w(1-\alpha)AU = m_w = \text{flow rate of water} \tag{25}$$

The flow rates of air and water are constant since steady flow was assumed.

All the properties are now known at $x+\Delta x$ and the process may be repeated until desired end conditions are obtained. In most cases the procedure was continued until the pressure reached atmospheric pressure. Numerical instability made the choice of Δx important. It was found that an initial value of 0.0001 ft was satisfactory in most cases; however, Δx must be decreased by an order of magnitude at a point where x is about two-thirds of the distance between the nozzle entrance and the throat. To prevent instability, this decrease in Δx must be divided into several increments. The exact location of the decrease in Δx is not of great importance as long as it is located far enough upstream to prevent the solution process from becoming invalid, and far enough downstream so that the time required for solution is not prohibitive. The instability is controlled by forcing the flow rates of air and water to be constant at each plane throughout the solution. This constrains the values of A and α at each increment. Sixteen significant digits were necessary to control the instability completely.

The exit velocities, U_e and V_e, and the exit pressure P_e were used in Eq. (16) to calculate the thrust produced by the waterjet.

Discussion of Results

The performance of a small air-augmented waterjet is analyzed for various input conditions. The conditions studied are: pump-outlet pressure, initial bubble radius, air injection temperature, mass ratio of air to water, and the heat transfer phenomena between the air and water. Specified input quantities are listed in Table 1.

Table 1 shows that some calculations were made for bubble void fractions of 0.005 and 0.01. At these void fractions conditions near the throat require interaction of the bubbles if the uniform bubble size model is retained. Thus, at these con-

Table 1 Specified input quantities used for analysis

l_o	(ft)	0.0833
P_a	(lbf/ft^2)	2100
P_{wi}	(lbf/ft^2)	7200; 9360; 10800; 12720; 14400; 17300; 20160; 23040; 28800
r_o	(ft)	0.00010; 0.00015; 0.00020; 0.00025; 0.00035; 0.00050; 0.00070
T_{gi}	(°R)	400; 500; 600; 800; 100; 1200; 1500
T_w	(°R)	530
U_a	(fps)	20
U_i	(fps)	20
V_i	(fps)	40
ν	...	0.001; 0.005; 0.010
water velocity profile		$U(x) = (\tanh(10x-3) + \tanh(3))100 + U_o$

ditions the model used contradicts reality. However, the uniform sphere assumption primarily affects the drag relation between air and water. Since the results show that the velocity of bubble and air approach each other at the higher void fractions, this interaction is negligible. Data presented in Ref. 11 confirms this observation.

Typical profiles of pressure, air temperature, air density, void fraction, bubble radius, air velocity, and nozzle radius are shown in Figs. 3 and 4. The abrupt change in the profiles of air density, bubble radius, and void fraction near the nozzle entrance is due to the rapid decrease in air temperature. The water has been assumed to be an infinite heat sink, which is very close to reality, and hence, the air bubbles cool rapidly to the temperature of the water. As the air cools, the bubbles shrink, and the air density increases since the water pressure and the pressure within the bubbles are equal at a cross-section of the nozzle. The number of bubbles crossing a plane in the nozzle is constant; hence, as the bubble radius decreases rapidly, the void fraction also decreases. However, after the air and water have reached thermal equilibrium, the bubbles begin to increase in size due to the negative pressure gradient within the nozzle. Simultaneously, the nozzle radius is decreasing, thus, the void fraction increases and the air density decreases. As the flow approaches the throat, a steep negative pressure gradient develops, thus, the bubbles grow more rapidly and, hence, more work is done on the water. The air and water velocity profiles, in nondimensional form, (see Fig. 3) appear to be almost coincident; however, there is a relative or slip velocity between the components. These curves do show that the velocity profile calculated for the air follows very closely the form of the velocity profile specified for the water.

The relationship of percent thrust augmentation and initial bubble radii is shown in Fig. 5 for several air injection temperatures. The effect of changing the initial bubble radius is significant only for initial bubble radii less than 0.00025 ft. The increase in thrust for the smaller initial size of the bubbles is observed because more bubbles are present to do work on the water. However, the model used in this analysis does not consider the effect of surface tension of the bubbles, and hence, is not valid for very small bubbles. Figure 6 shows bubble radius profiles for several runs where only the initial bubble radius was different. There is very little difference in the nondimensional profiles. In fact, for initial bubble radii larger than 0.00025 ft, the curves are coincident.

Figure 7 shows the effect of mass ratio on the percent thrust augmentation for different air injection temperatures. Both the two-phase thrust and the percent thrust augmentation increase with an increase in mass ratio. The thrust produced is only weakly dependent on the air injection temperature. The small increase in thrust at high air injection temperatures is due to slightly higher velocities, of both the air and water, and an increase in void fraction at the mixing chamber exit.

The percent thrust augmentation is shown in Fig. 8 as a function of the ratio of pump-outlet pressure to back pressure for different mass ratios and air injection temperatures. The percent thrust augmentation will approach infinity as the pump-outlet pressure goes to zero, and will approach zero as the pump-outlet pressure increases. This occurs because the thrust of the water goes to zero as the pump-outlet pressure goes to zero, but there remains a finite thrust due to the air alone. Also, as the pump-outlet pressure increases, the void fraction at the mixing chamber exit decreases, and since the bubble radius is predetermined, the number of bubbles decreases and less work is done on the water.

The water has been assumed to be an infinite heat sink, hence, the temperature of the air rapidly approaches the temperature of the water. Three different models of heat transfer from the air to the water have been considered. The first model is the adiabatic bubble model; no heat transfer to the water. The second model is an intermediate model in which there is a finite heat transfer between the air and water. This

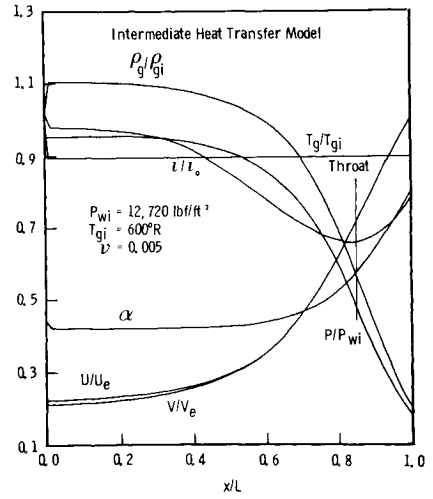

Fig. 3 Typical profiles of α, and ρ_g, P, T_g, nozzle radius, air velocity and specified water velocity profile.

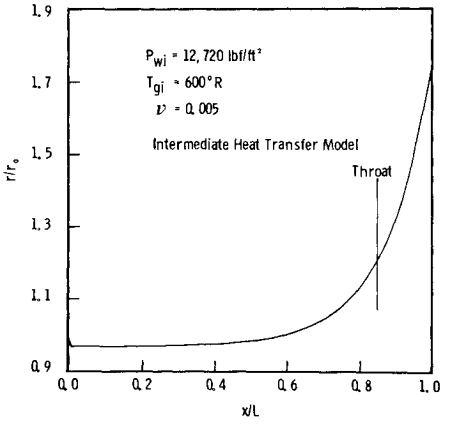

Fig. 4 Typical bubble radius profile.

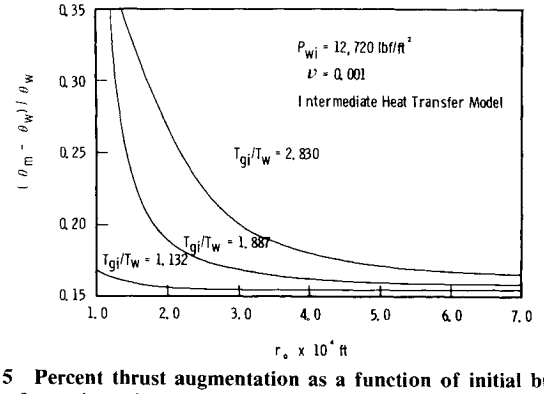

Fig. 5 Percent thrust augmentation as a function of initial bubble radius for various air injection temperatures.

model is based on empirical results, Eq. (9). The third model is the isothermal bubble model; the air immediately assumes the temperature of the water. Figure 9 shows the percent thrust augmentation as a function of the ratio of air injection temperature to water temperature. The predicted thrust is not affected greatly by the heat transfer model used, at least over the range of T_{gi}/T_w from 1.0-2.0. At the lower mass ratios the effect of the different heat transfer models is less pronounced. The air temperature profile is different for the adiabatic bubble model than for the intermediate model or the isothermal bubble model. Figure 10 shows typical air temperature profiles for the different heat transfer models. The adiabatic bubble model does not have an abrupt change in air tem-

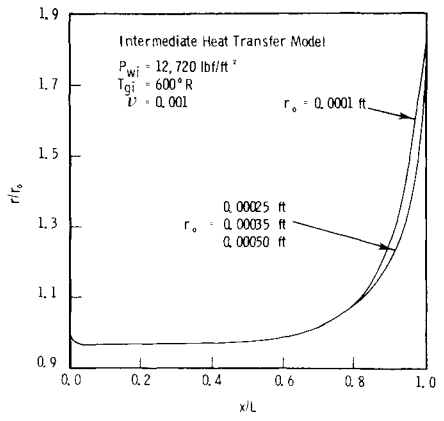

Fig. 6 Bubble radius profiles for different initial bubble radii.

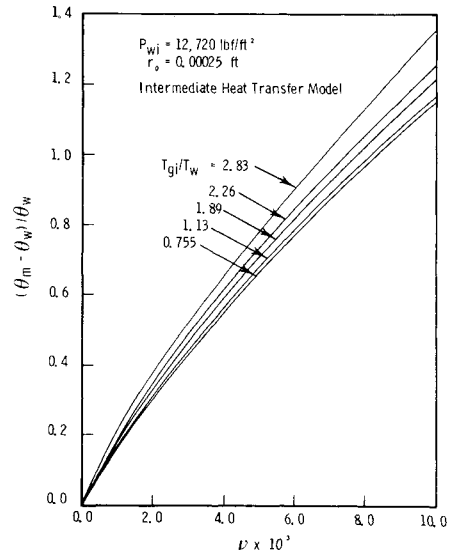

Fig. 7 Percent thrust augmentation as a function of mass ratio for various air injection temperatures.

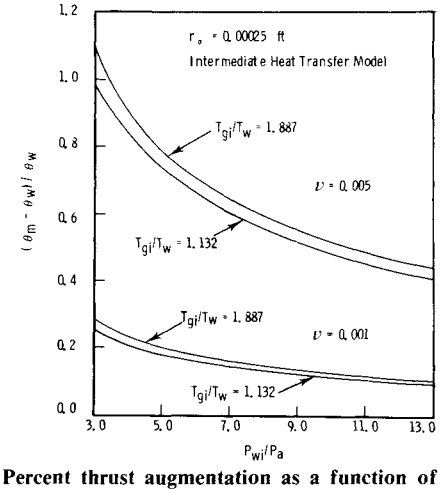

Fig. 8 Percent thrust augmentation as a function of pump-outlet pressure for various air injection temperatures and mass ratios.

perature initially as do the other models. With the adiabatic bubble model the air is cooled only by the expansion of the bubbles. The air temperature drops below the water temperature because no heat can be transferred from the water to the bubbles during the rapid expansion through the latter portion of the nozzle. The intermediate model and the isothermal bubble model so closely coincide that only the intermediate model and the adiabatic bubble model need be considered.

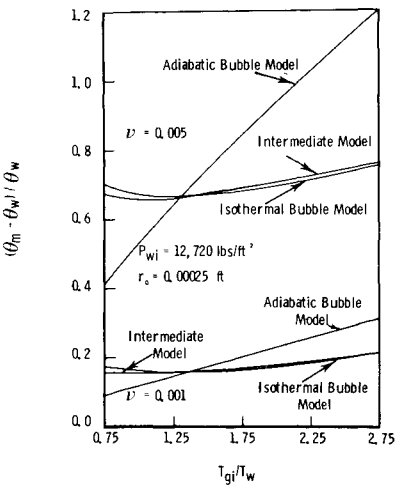

Fig. 9 Percent thrust augmentation as a function of air injection temperature for the different heat transfer models.

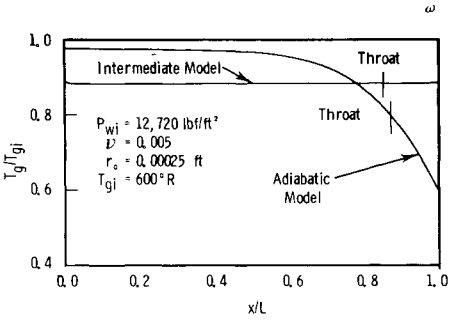

Fig. 10 Typical profiles of T_g for adiabatic bubble model and intermediate model.

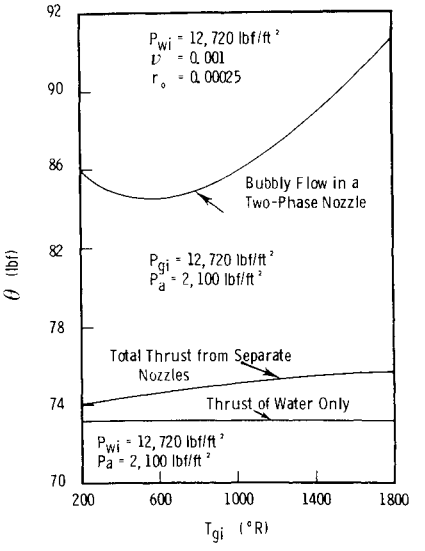

Fig. 11 Comparison of thrust of two-phase nozzle and combined thrust of separate nozzles for the air and water.

Figure 11 is a comparison of the thrust produced by a two-phase nozzle and the sum of the thrusts of 2 nozzles in which the air and water are flowing separately. In calculating the thrust of the separate nozzles, both the air and the water are assumed to expand isentropically. The separate air nozzle produces a very small thrust due to the small flow rate of air. For the cases compared in Fig. 11, there is 13% more thrust, at an initial air temperature of 600°R, from the two-phase nozzle than from the two separate nozzles.

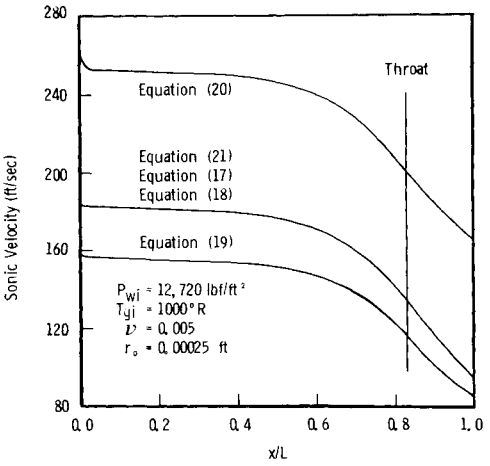

Fig. 12 Sonic velocity profiles.

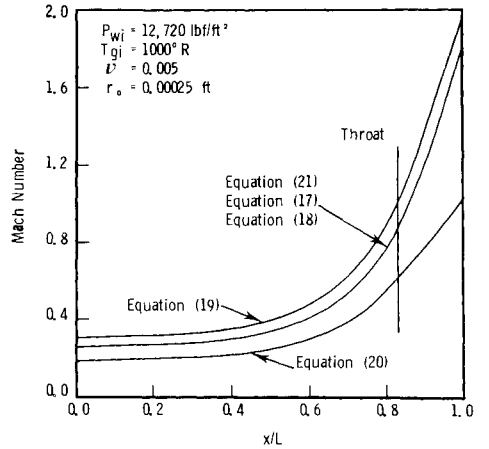

Fig. 13 Mach number profiles.

The sonic velocity profiles predicted by Eq. (17-21), for a typical run, are shown in Fig. 12. The Mach number profiles, calculated by Eq. (22) for each of the sonic velocity profiles, are compared in Fig. 13. Van Wijngaarden's first approximation, Eq. (19), produces a Mach number nearest unity at the minimum area section. Equations (17, 18, 21) predict essentially the same Mach number profiles, however, they do not predict a Mach number of unity at the minimum area of the nozzle.

Conclusions

It is concluded that the injection of air into the flow through a waterjet can produce a significant increase in the thrust developed by the system. However, when a fixed nozzle geometry is specified, the flow rate of water through the nozzle decreases as the flow ratio of injected air increases, thus there is a decrease in thrust due to the decrease in the flow rate of water. Thrust augmentation from the injection of air into the flow is great enough for some conditions to produce an appreciable net increase in thrust for the system.

The thrust augmentation is only weakly dependent on the air injection temperature. Thus, there is very little advantage in heating or cooling the air before injection into the water stream. This simplifies the analysis of the air-augmented waterjet, since for air injection temperatures near the water temperature, the heat transfer phenomena between the air and water makes very little difference in the thrust produced.

Increasing the ratio of mass flow rate of air to mass flow rate of water, within the bubbly flow regime, accounts for the greatest increase in thrust augmentation, whereas, the increase of pump-outlet pressure decreases the thrust augmentation. Hence, a lower pressure system which moves a large mass of water and a relatively high mass ratio would produce the greatest thrust augmentation. Injecting air into the flow of a waterjet produces much more thrust augmentation than does flowing the air and water in separate nozzles.

Only one expression for sonic velocity of the mixture yields a Mach number close to unity at the minimum area of the nozzle. The accuracy with which this expression predicts a Mach number of unity at the minimum area section depends on the input conditions, in particular on the ratio of air injection temperature to water temperature. Hence, more study is needed to develop an expression which will consistently predict a Mach number of unity at the minimum area section.

References

[1] Amos, R. G., Maples, G., and Dyer, D. F., "Thrust of an Air-Augmented Waterjet," *Journal of Hydronautics,* Vol. 7, April 1973, pp. 64-71.

[2] Vliet, G. C. and Leppert, G., "Forced Convection Heat Transfer from an Isothermal Sphere to Water," *Journal of Heat Transfer,* Vol. 83, 1961, pp. 163-175.

[3] Schlichting, H., *Boundary Layer Theory,* McGraw-Hill, New York, 1968, p. 108.

[4] Bird, R. B., Stewart, W. E., and Lightfood, E. N., *Transport Phenomena,* Wiley, New York, 1960, p. 192.

[5] Haberman, W. L. and Morton, R. K., "An Experimental Investigation in the Drag and Shape of Air Bubbles Rising in Various Liquids," David Taylor Model Basin Rept. 802, NS 715-102, Sept. 1953, Washington, D.C.

[6] Kreith, F., *Principles of Heat Transfer,* International Textbook Co., Scranton, Pa., 1965, pp. 595-597.

[7] Keenan, J. H. and Kaye, J., *Gas Tables,* Wiley, New York, 1945.

[8] Wallis, G. B., *One-Dimensional Two-Phase Flow,* McGraw-Hill, New York, 1969, pp. 244-246.

[9] Van Wijngaarden, L., "One-Dimensional Flow of Liquids Containing Small Gas Bubbles," *Annual Review of Fluid Mechanics,* Palo Alto, Calif., Annual Reviews, Inc., 1972, pp. 369-396.

[10] Henry, R. E., Grolmes, M. A., and Fauske, H. K., "Propagation Velocity of Pressure Waves in Gas-Liquid Mixtures," *Concurrent Gas-Liquid Flow,* Plenus Press, New York, 1969, pp. 1-18.

[11] Maxwell, T. T., Stansell, J. F., Maples, G., and Dyer, D. F., "Performance of Gas-Augmented Water Jet Propulsion System," ONR Contract N00014-72-C-0177, Sept. 1973, Office of Naval Research, Washington, D.C.